Journal of Petroleum Science and Technology 11(4): 32, 2021, Pages 2-13
DOI:10.22078/JPST.2022.4683.1772

Journal of Petroleum Science and Technology
Research Peaper
https://jpst.ripi.ir/

Analysis of Liquid Bridge Characteristics in a Horizontal Fracture: Critical Fracture Aperture and Fracture Capillary Pressure

Sadegh Dahim, Behrouz Harimi*, Mohammad Hossein Ghazanfari and Mohsen Masihi
Chemical and Petroleum Engineering Department, Sharif University of Technology, Tehran, Iran

Abstract
The liquid bridge is considered a good means to maintain capillary continuity between overlying matrix blocks if its stability in fractures is preserved. Despite several studies focusing on the liquid bridge in different environments, little attention is paid to dig through a single liquid bridge between thin sections of minerals found in fractured reservoirs. In this study, a set of experiments was conducted to investigate liquid bridge stability and surface profile for different values of liquid volume and surface wettability conditions. It is found that critical fracture aperture is linearly proportional to the contact angle and to the third root of liquid volume, which is depicted by a newly developed expression. An accurate method for computation of capillary pressure of liquid bridge (known as fracture capillary pressure) from the experimentally determined interface profiles, based on the numerical solution of the Young-Laplace equation, is proposed. Following the Plateau sequence, both nodoid and unduloid shape bridges are observed with an increase in fracture aperture, corresponding to positive and negative fracture capillary pressure, respectively. It is interesting to note that instability of liquid bridges occurs at small negative values of capillary force where some attraction force exists between fracture faces. By applying a 1D mathematical model of liquid dripping, a modified expression for the prediction of critical fracture aperture is proposed, including fluid and flow-related parameters. The findings of this study help to better incorporate the role of liquid bridge and corresponding fracture capillary pressure in capillary continuity in fractured porous media.

Keywords: Liquid Bridge, Capillary Bridge, Capillary Continuity, Critical Fracture Aperture, Fracture Capillary Pressure, Experimental, Theoretical.

Introduction
Predicting the gravity drainage performance in naturally fractured reservoirs using the assumption of independent matrix blocks is far from reality. Block to block interaction affects the recovery rate and ultimate recovery of gravity drainage through re-infiltration and capillary continuity phenomena. Both phenomena are controlled by the geometrical and petrophysical properties of the matrix and fracture media and oil and gas properties. Reinfiltration of drained oil from upper matrix blocks into the lower ones has been investigated by both experimental and modelling studies [1-5]. On the other hand, establishing capillary continuity between a stack of matrix blocks improves the ultimate recovery due to the enhanced effective height of the oil column. The liquid bridge formation in the fracture is believed to be a promising way to establish capillary continuity between overlying matrix blocks. When a liquid body is introduced in the space between two solid surfaces or between a solid and a liquid surface, a liquid bridge might be formed, provided that the spacing between solid bodies is sufficiently small [6]. This phenomenon is pertinent to many scientific and industrial applications such as experiments with atomic force microscope [7-12], medical and cell culture science [13-15], studies of granules [16-19], particle adhesion [20-22], nanoscale applications [23, 24], and water saturation in soil [25-27] as well as oil recovery from fractured reservoirs [28, 29]. Although several authors investigated liquid bridges with the aid of experiments and theoretical models, little attention has been given to the liquid bridge formation, stability, and related characteristics and its contribution to maintaining capillary continuity in fractured porous media. The liquid bridge could also affect reinfiltration process since it provides a path of liquid transfer between neighboring matrix blocks. The solution of Young-Laplace equation was applied to propose a theoretical model for fracture capillary pressure in the

**Corresponding author:* Behrouz Harimi, Chemical and Petroleum Engineering Department, Sharif University of Technology, Tehran, Iran
E-mail addresses: behrouz.harimi@alum.sharif.edu
Received 2022-03-14, Received in revised form 2022-04-06, Accepted 2022-04-10, Available online 2022-09-05

presence of liquid bridges by Firoozabadi and Hauge [30]. Fracture capillary pressure curves were presented by assuming different fracture geometries by them. Firoozabadi and Markeset [3] monitored the process of liquid bridge formation and breakage inside the fractures in the course of gravity drainage experiments of stacked blocks. They reported that liquid bridges in the upper fractures become unstable earlier than the lower fractures. Based on the results of their laboratory experiments of gravity drainage, it has been argued by Sajadian et al. [4] that when fracture aperture is less than a critical value, liquid bridges are formed and then effective capillary continuity is provided. The stability of liquid bridges in fractured porous media at the pore scale using a glass micromodel representing a stack of two blocks was studied by Mashayekhizadeh et al. [31]. They investigated the stability and frequency of the liquid bridges versus time and at different tilt angles. Dejam and Hassanzadeh [32] proposed a model describing the elongation and subsequent breakup of a liquid element suspended from a horizontal surface. Their work could depict the formation process of liquid bridges but not the bridge characteristics after its formation. found a relationship between the net capillary force, contact angle, and liquid bridge volume to examine the stability of a liquid bridge between two horizontal plates in the absence of gravity was found by Dejam et al [33]. A map by combination of a range of values of contact angle and dimensionless liquid bridge volume to display three possible regions, namely: liquid bridge break-up, liquid bridge formation and nonexistence was developed by them. Furthermore, free surface flow equations and the concept of minimum Gibbs free Energy to analyze the static stability of liquid bridge in fractures were applied by Miri et al [34]. They found a relationship for critical length of liquid bridge as a function of pore throat size. In addition, models of rough-walled fractures representing different geometrical characteristics of natural fractures were introduced by Harimi et al [28]. Then, they presented a comprehensive analysis of liquid bridge stability and related capillary pressure in the proposed rough-walled fracture models. Furthermore, mathematical expressions for the prediction of liquid bridge stability and fracture capillary pressure as a function of liquid saturation, fracture aperture and surface roughness and wettability conditions are proposed. A “3D-fracture, 2D-matrix” micromodel for visual analysis of liquid bridge in gas-liquid gravity drainage process was utilized by Bina et al. [35]. Also, they emphasized the validity of the Young-Laplace equation to evaluate fracture capillary pressure. More recently, a mathematical model to describe the required conditions for liquid bridge formation from dripping liquid threads in fractures was applied by Harimi et al. [36]. They found out that the fracture capillary pressure in the presence of a liquid bridge is considerably greater than that of suspended liquid drops.

To determine whether a stable liquid bridge could be formed, the concept of maximum or critical rupture distance is helpful. The critical rupture distance aperture is defined as the maximum value of the distance between the solid substrates that an embedded liquid drop with a given volume may form a stable liquid bridge. Similarly, in the liquid bridges in natural fractures, critical fracture aperture refers to the maximum fracture aperture that could retain a liquid bridge. The curvature of the gas-liquid interface of the liquid bridge induces a pressure difference across the interface, which is known as capillary pressure [37].

This capillary pressure affects the total capillary force between the solid bodies supporting the liquid bridge, which is important in several processes related to partially wetted particles. Due to the existence of a liquid bridge, capillary pressure controls the fracture capillary pressure that quantifies the degree of capillary continuity between two matrix blocks embracing the fracture. Numerical simulation results of Dindoruk and Firoozabadi [38] revealed that the least capillary pressure contrast between fracture and matrix produced the highest amount of oil from matrix blocks. Furthermore, the role of fracture capillary pressure models on the oil recovery by applying fine-grid numerical simulation was analyzed by Dejam [39]. They found that both constant and saturation-dependent fracture capillary pressure improves ultimate recovery compared to zero capillary pressure. Still, the amount of recovery enhancement depends on the capillary pressure model. According to the importance of fracture capillary pressure, vigorous methods are required to predict this parameter, as highlighted in the abovementioned studies.

Evaluation of critical fracture aperture and fracture capillary pressure, as the two important features of the liquid bridge for application of our interest, is the main goal of this study. To this end, a laboratory setup is designed to create and visualize micro scale liquid bridges between two parallel plates, representing the faces of a horizontal fracture. Several experiments were conducted, and the results were analyzed with mathematical formulations to obtain the desired characteristics of the liquid bridge. Furthermore, mathematical formulations are applied to interpret the desired characteristics of liquid drops and liquid bridges from experimental results.

Materials and Methods

In this section, the experimental setup and procedure are presented first. Then, the methods of numerical analysis of experimental data as well as evaluation of fracture capillary pressure by a novel scheme is discussed.

Experimental Setup and Materials

An experimental setup was designed to observe and measure the characteristics of liquid bridges at the micro scale. A detailed schematic diagram of the setup is shown in Figure 1. This setup is mainly made up of two plates attached to a mainframe. A rectangular blank is inserted on each of the plates to install the desired solid substrates, including glass and thin sections of porous rock. The solid substrates must be cleaned with proper solvents and dried accordingly before every test. The lower plate is stagnant, but the upper one is movable, and it can do a vertical translation with an accuracy of 4 micrometers. A D-SLR D90 Nikon digital camera equipped with a macro reversing ring was used to capture images and check the parallelism of inserted solid substrates. A light source is included to obtain sufficient contrast to visualize the liquid bridge.

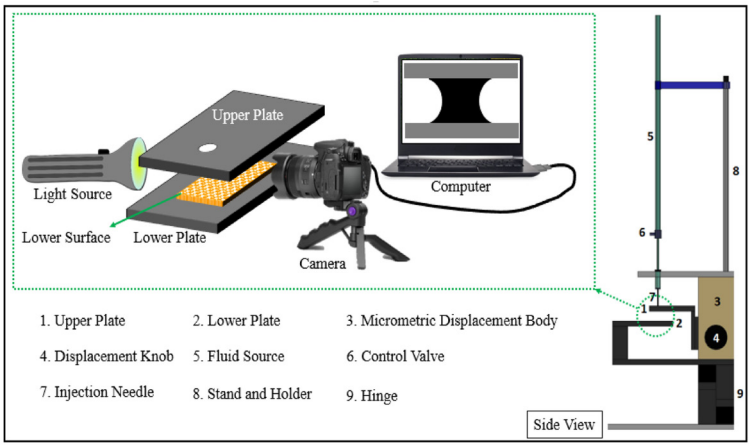

Fig. 1 Schematic of the apparatus.

Experimental Procedure

The aim of the conducted experiments is to investigate the stability and some characteristics of the formed liquid bridges. The obtained data are then used to determine critical fracture aperture and fracture capillary pressure pertinent to capillary continuity in fractured porous media. To create a liquid bridge, a drop with a specified volume is placed on the lower plate using a micropipette with an accuracy of 0.5 microliters. Then, the upper plate is lowered toward the drop until a liquid bridge is formed. After creating the liquid bridge, the upper plate is moved upward slowly in several steps, and images of the liquid bridge are recorded at each step. This process continues until the breakage of the bridge. The liquid bridge formed during the described procedure is called a "static" liquid bridge which refers to the inexistence of dynamic effects. In other words, no liquid flows through the bridge and sufficient time is given to the bridge after each change in fracture aperture to stabilize any motions. These static conditions usually conform to the behavior of naturally fractured carbonate reservoirs due to their low matrix permeability and, in consequence, small drainage rates. Thereafter, the role of viscous force on the stability and capillary pressure of the liquid bridge is usually a trial. In Table 1, the description of the conducted experiments is provided. The liquid bridge volume formed in fracture could be conceived as a measure of liquid saturation in fracture during the gravity drainage process. Hence, a sensitivity analysis of the effect of liquid volume on the stability and capillary pressure of the bridge is helpful. According to Table 1, glass slides were used as substrates in the first set of experiments as a base case, representing smooth water-wet sandstone surfaces. However, porous materials made from carbonate minerals, commonly found in naturally fractured reservoirs, had better be used as representative of natural fractures. In this respect, thin sections of calcite were used as solid substrates in the next set of experiments. In addition, to evaluate the role of surface wetness on the stability and other features of liquid bridge, two experiments were conducted using calcite sections treated with a mixture of crude oil and stearic acid. It has been shown that this treatment tends to shift the liquid wetting of the surface toward a gas wetting state [40, 41]. The measured equilibrium contact angle of water drop on a glass slide, calcite and treated calcite are 46, 61 and 76 degrees, which the values show water-wet, weakly water-wet and neutral wet conditions, respectively. To ensure the experimental repeatability and diagnose any possible fault in the experimental procedure, tests # 3 and 7 were repeated two more times.

Evaluation of Liquid Bridge Characteristics

An open-source image processing software, ImageJ®, was applied for extracting geometrical characteristics of the liquid bridge, i.e. length (fracture aperture), neck radius, and gas-liquid-solid contact radius from captured images, as shown in Figure 2. Since, in each test, the fracture aperture increases stepwise until the rupture of the bridge, the final fracture aperture just before rupture is considered the critical fracture aperture. To compute capillary pressure from liquid bridge interface profile, a new numerical procedure has been proposed based on the exact solution of the Young-Laplace equation, as depicted in the next section.

Table 1 Details of conducted static liquid bridge experiments.

Test #	Solid Substrate	Liquid Volume (µl)	Initial (equilibrium) contact angle
1	Glass	5	46
2	Glass	10	46
3	Glass	20	46
4	Calcite	5	61
5	Calcite	10	61
6	Calcite	20	61
7	Calcite treated by stearic acid	5	76
8	Calcite treated by stearic acid	10	76

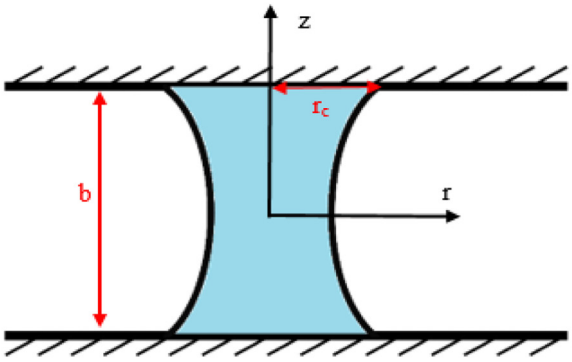

Fig. 2 Schematic profile of liquid bridge.

Fracture Capillary Pressure

Young-Laplace Equation, known as the basic equation of capillarity, states that the mean curvature of a free meniscus is proportional to the pressure drop across the meniscus interface. According to the Young-Laplace equation, the capillary pressure of a meniscus is controlled by its two principal radii of curvatures [37].

Two types of liquid bridge, *namely θ-bridge* and *r-bridge*, were distinguished by Fortes et al. [42]. In the former one, the solid contact radius is controlled by the contact angle and volume of the liquid bridge. In contrast, for the r-bridge types, the contact radius is fixed, but the volume of the bridge adapts to the contact angle. For the application of our interest, i.e. formation of the liquid bridge in fractures between overlying matrix blocks, the size of the liquid bridge is considerably smaller than the surface area of a matrix block. Hence, only *θ-bridge* are expected to appear in fractures. The following equation for obtaining the interface profile of liquid bridge, z(r), based on the Young-Laplace equation, was derived by Fortes et al. [42]:

$$Z(R) = \int_{R_c}^{R} f(R)[1 - f^2(R)]^{-0.5} dR \quad (1)$$

where f(R) is defined as follows:

$$f(R) = \frac{R_0 + \beta R_0^2}{R} - \beta R \quad (2)$$

where dimensionless parameter β is defined as $\beta = Pr_c/2\sigma$. In this equation, rc is the radius of the three-phase contact line, $Z=z/r_c$ and $R=r/r_c$ are dimensionless coordinates, R_0 is dimensionless neck radius, P_c is capillary pressure, and σ is surface tension. All required data for Equations 1 and 2 except capillary pressure are directly determined from digitized, recorded images. To find the accurate capillary pressure for a liquid bridge with known profile, a new procedure is developed, as described in Figure 3. According to this procedure, an initial value of capillary pressure is guessed, and the profile of the liquid bridge is obtained from Equation 1. Then, it is compared with the experimentally determined profile. The toroidal approximation can be applied to make a reasonable estimate of capillary pressure. Suppose the guessed value did not lead to a reasonable match. In that case, the value of capillary pressure is iteratively modified to improve the match between the numerically calculated and experimentally determined profile of liquid bridge. The obtained value of capillary pressure at the end of this iterative process is a reliable prediction of fracture capillary pressure that conforms to experimental results and satisfies the exact solution of the Young-Laplace equation.

Results and Discussions

Liquid Bridge Profile

As mentioned in section 2, the liquid bridge images are recorded to extract different features of the liquid bridge. The sequential photographs of the liquid bridge with increasing fracture aperture are depicted in Figure 4. The rightmost photo in each row shows the liquid bridge in critical condition, i.e. just before rupture. Analysis of the evolution of neck radius, contact radius, instantaneous contact angle and interface profile of liquid bridge are extractable features of the liquid bridge for different uses. For the application of our interest, i.e. capillary continuity, the curvature of the interface profile of the liquid bridge that determines the capillary pressure is the most important one.

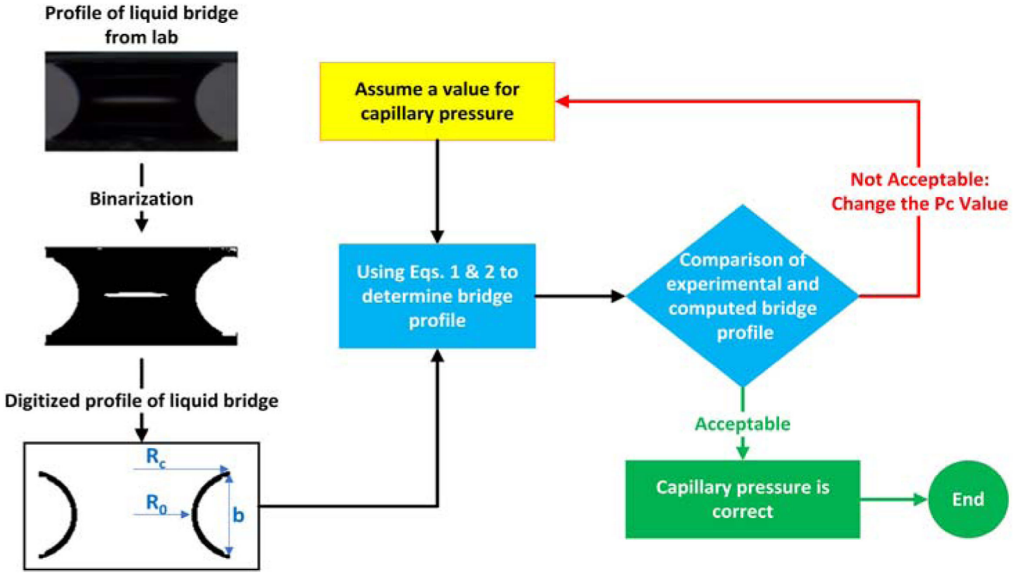

Fig. 3 Flowchart of the proposed method to calculate the fracture capillary pressure from experimentally measured profile of liquid bridge.

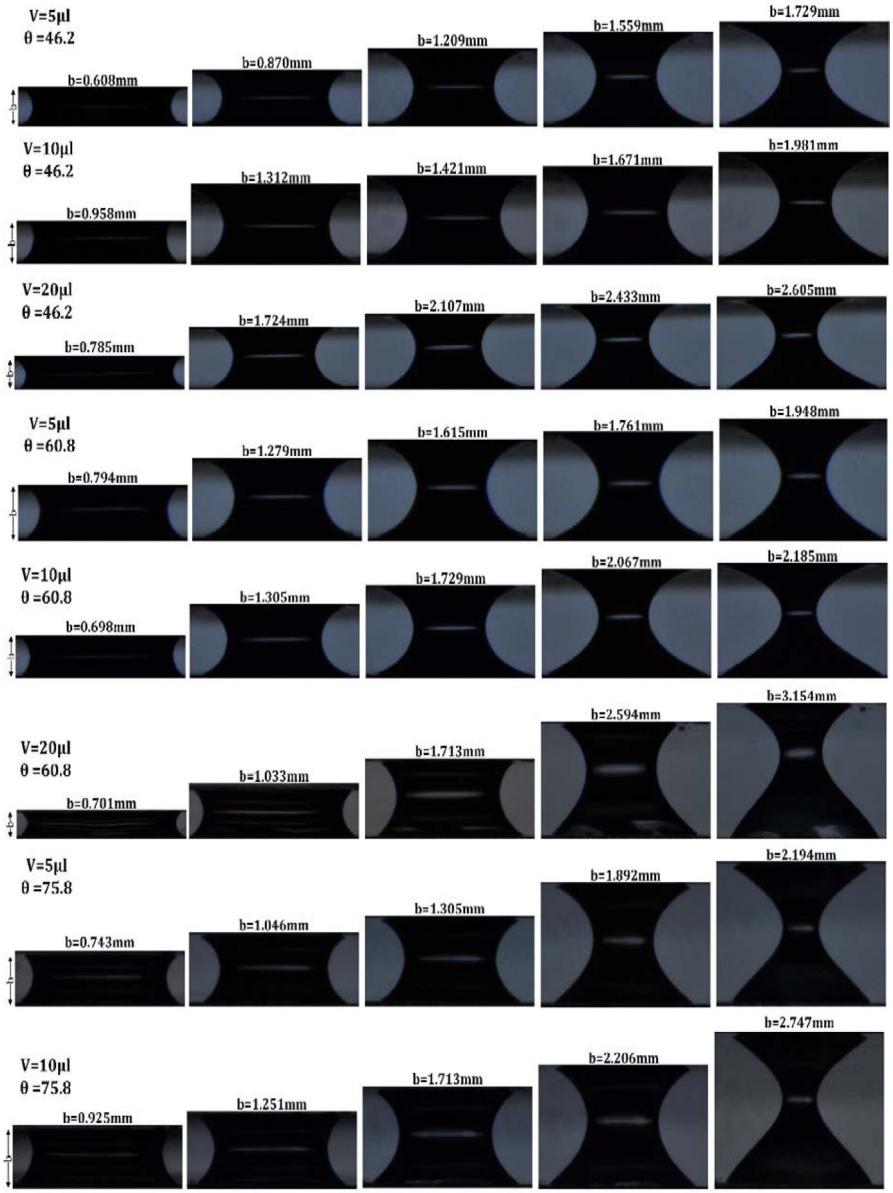

Fig. 4 Sequensive images of liquid bridges with increasing fracture aperture until rupture.

In Figure 5, the variation of neck radius by increasing fracture aperture for different surface wetness conditions. Each plot corresponds to a given volume of the liquid bridge, and the rightmost point in each curve denotes the neck radius and fracture aperture just before rupture. Treatment of calcite with a solution of stearic acid in chloroform is successfully applied to obtain a hydrophobic surface. By increasing contact angle, the curves are slightly shifted to the right, meaning that lower surface wetness remediates the reduction of neck radius due to increased fracture to some extent. This observation was previously noted in the modelling results of Harimi et al. [28]. As a result, greater values of contact angle lead to an increase in the critical fracture aperture. Moreover, it can be observed that there is a critical value for the neck radius at the moment of instability of the liquid bridge, and it does not approach zero at the rupture moment.

In Figure 6, the repeatability of some experimental results is illustrated. As indicated in this figure, the evolution of neck radius by increasing fracture aperture is identical for three different runs, which assures us about the precision of the experiment and data acquisition procedure.

Critical Fracture Aperture

Critical fracture aperture could be considered an important measure to estimate the significance of capillary continuity in a fractured porous media. Comparing the critical fracture aperture with the distribution of average fracture aperture in the reservoir reveals whether liquid bridge formation is expectable or not. In Figure 7, the role of contact angle and liquid volume on the experimental measurements of critical fracture aperture is illustrated. It can be seen that critical fracture aperture increases linearly with contact angle. As noted in the previous section, with increasing contact angle, the liquid is partly shifted from supporting plates to the center of the bridge. As a result, the neck radius gets thicker by increasing the contact angle, enabling the bridge to be stable at greater values of fracture aperture.

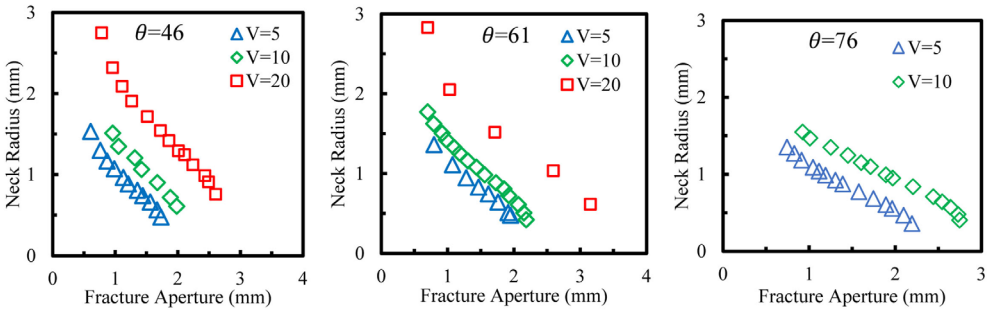

Fig. 5 The effect of liquid volume on the evolution of neck radius with increasing fracture aperture in constant wettability state (Volume and contact angle are in µL and degree, respectively.)

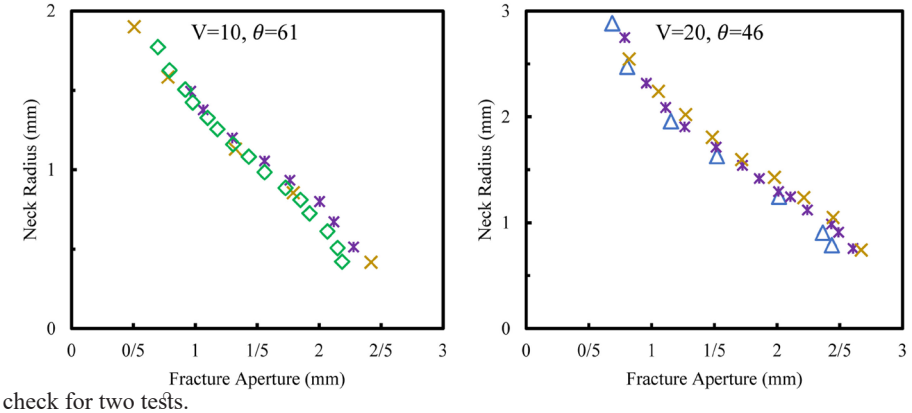

Fig. 6 Repeatability check for two tests.

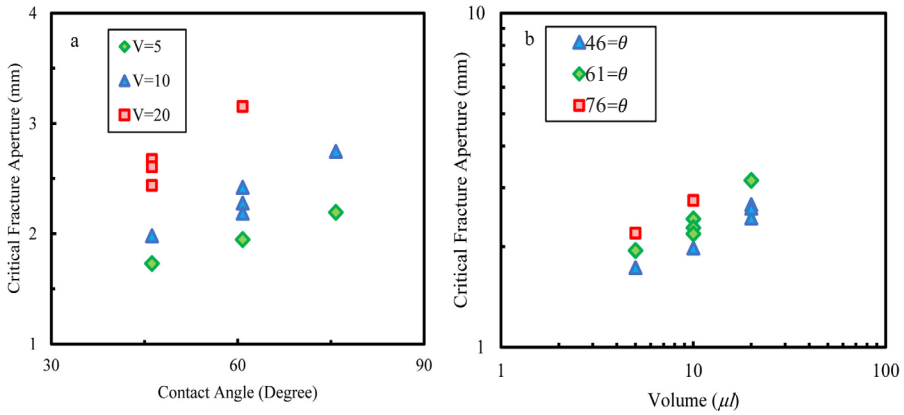

Fig. 7 Critical fracture aperture as a function of: a) Contact angle in a constant liquid bridge volume and b) Liquid bridge volume in a constant contact angle.

On the other hand, critical fracture aperture is almost proportional to the third root of liquid bridge volume at a given contact angle. For the case of a liquid bridge between two spheres, Lian et al. [43] presented an expression that relates dimensionless separation distance to the third root of dimensionless bridge volume. This functional relationship between critical fracture aperture, liquid bridge volume and contact angle inspired us to derive a mathematical relationship for the case of the liquid bridge in horizontal fractures, i.e. bridge between smooth plates. According to the obtained experimental dataset, the following expression is proposed for predicting the critical fracture aperture. The constant values are determined from the best regression fit (R^2=0.929).

$$b_c = 0.46(1+1.37\theta)V^{1/3} \quad (3)$$

where θ is the contact angle (in radian) and V is the drop volume (μL). Computed values of critical fracture aperture from Equation 3 and experimentally measured values are shown in Figure 8, indicating a great match. If adequate information about geometrical features of the fracture system is available, Equation 3 could be utilized for fast screening the probability of liquid bridge formation in that reservoir. This helps us recognize whether the liquid bridge is the dominating mechanism of fracture capillary pressure or not. Otherwise, direct contact of matrix blocks and film formation over non-porous materials in fracture are alternatives to control fracture capillary pressure. It is worth mentioning that Equation 3 is derived using a limited number of experimental data, i.e. eight data points after excluding repeatability tests. Hence, supplementary experiments might be required to adjust the values of regression coefficients, i.e. 0.46 and 1.37.

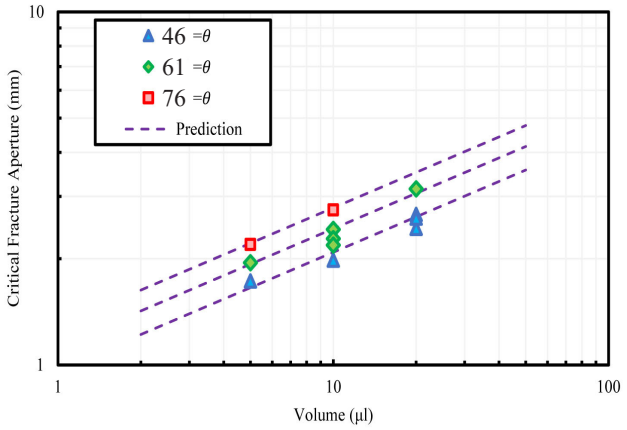

Fig. 8 Comparison of the experimentally measured critical fracture apertures with the calculated values using Equation 3.

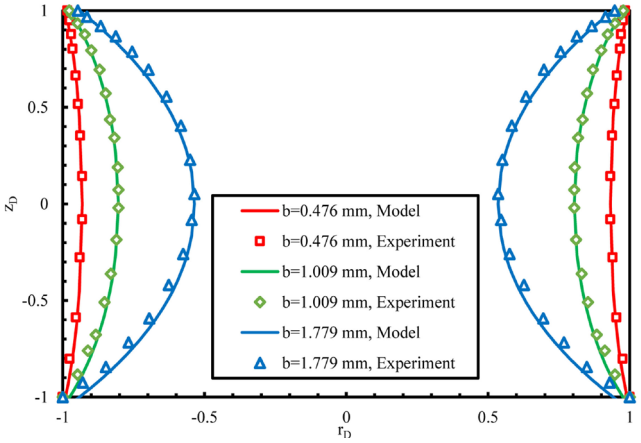

Fig. 9 Examples of an acceptable match between experimental and model interface profile of liquid bridge.

Fracture Capillary Pressure

As described earlier, a new method is used to calculate fracture capillary pressure from the digitized interface profile of liquid bridge photographs. Figure 9 shows examples of an acceptable obtained match between the measured profile of the bridge and the numerically computed profile used to calculate the capillary pressure of the liquid bridge from its profile. This approach shows the capillary pressure for the liquid bridge with given liquid volume, aperture and wettability condition from its observed interface profile. The advantage of this method is to use the exact form of the Young-Laplace equation instead of the well-known approximation method, e.g. toroidal approximation. The calculated capillary pressure of the liquid bridge could be attributed to the fracture's capillary pressure, including the bridge.

Figure 10 presents the evolution of fracture capillary pressure with an increase in fracture aperture for different surface wettability conditions and liquid volumes. Initially, positive values of capillary pressure are found for lower fracture apertures. Then, by increasing fracture aperture, i.e. wider fractures, a transition from positive to negative capillary pressure is observed. This observation is in accordance with the results of Plateau [44], who distinguished the shapes of the capillary bridges by decreasing capillary pressure. Three shape sequences of the liquid bridge, which have a neck, namely nodoid with neck, catenoid and unduloid with neck, were introduced by Plateau [44]. As can be seen in Figure 10, the presence of a neck in a liquid bridge does not necessarily mean a positive capillary pressure. Figure 10b indicates that for greater values of liquid volume in fracture, the stability is improved, and the fracture capillary pressure increases to some extent.

However, it seems that this trend might reverse in lower fracture apertures. In other words, in thicker fractures, capillary pressure increases with an increase in bridge volume while in thinner aperture such trend is not observed. On the other hand, fracture capillary pressure decreases sharply with increased fracture aperture in all cases. Furthermore, it can be seen that contact angle does not affect fracture capillary pressure noticeably. However, this argument must be validated for a wider range of wettability conditions.

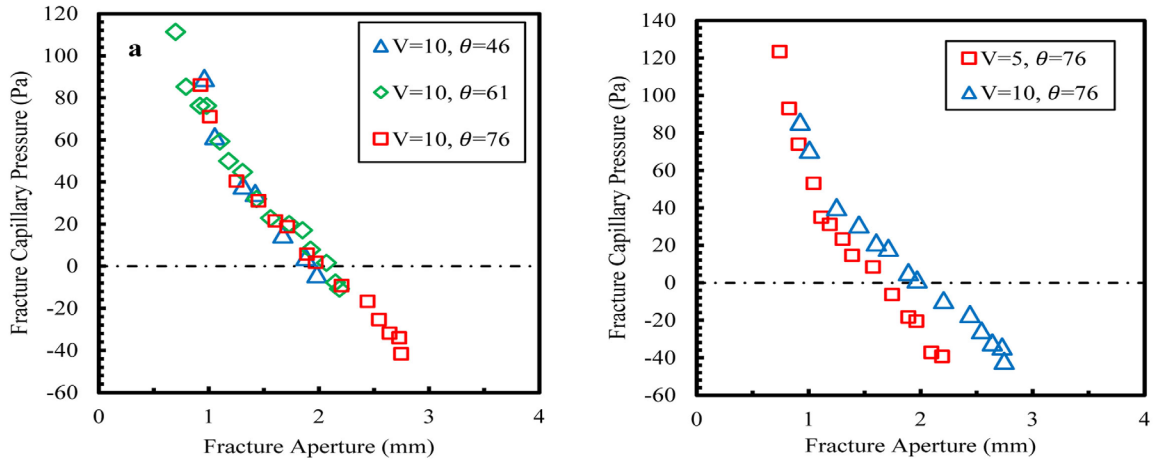

Fig. 10 Fracture capillary pressure versus fracture aperture: (a) role of contact angles and (b) role of liquid volume.

The abovementioned method for deriving the capillary pressure of a liquid bridge from its profile is based on the numerical solution of the exact form of the Young-Laplace equation. Instead of the exact solution of the Young-Laplace equation, several authors used a toroidal approximation to obtain simple relationships to determine the liquid bridge interface shape and capillary force. By this approximation, the surface of the liquid bridge is fitted on an arc of a circle. Hence, the meniscus is described as a part of a toroid [45]. In some cases, like nodoid shape liquid bridges, when the contact angle is between 70 to 90 degrees, the toroidal approximation equals the exact profile of the liquid bridge. The outer radius is determined by applying toroidal approximation by passing a circle from the neck radius and the two contact radii. On the other hand, there are some ambiguities in the definition of the inner radius in the published literature. The three common definitions for the inner radius are: $r_i=\frac{r}{\sin\theta}$, $r_i=r_c$ and $r_i=r_0$. The first and the third definitions correspond to the maximum and minimum possible values of the inner radius, and the second one is considered an intermediate value. Figure 11 compares the capillary pressure computed by the Young-Laplace equation with capillary pressure estimated by toroidal approximation using three definitions for inner radius. According to Figure 11, the differences between approximate and exact solutions are small, but with an increase in fracture aperture, the deviation of approximate solutions from the exact ones is accentuated.

Since none of the above-proposed approximations of inner radius could reasonably predict the actual capillary pressure, the definition of a new inner radius could be helpful. The following functional form might be used:

$$r_i^* = \alpha r_0 + (1-\alpha) r_c \quad (4)$$

where α is a regression coefficient ranging between 0 and 1. Using the newly defined inner radius and obtained capillary pressure values, an alpha coefficient was found for the best fit between obtained capillary pressure and toroidal approximation. Figure 12 shows the calculated α coefficient versus dimensionless capillary pressure, where it is defined as $P_c\, r_0/2\sigma$. Two distinct shape zones are separated according to the shape sequences of Plateau [44], namely nodoid and unduloid. For lower values of fracture aperture, nodoid-shaped liquid bridges are observed, whereas, by increasing fracture aperture and consequent decrease in capillary pressure, a transition to the unduloid-shaped bridge is seen. In nodoid zone, the α coefficient is almost one, but with switching to unduloid zone, α decreases. For the application of our interest, i.e. capillary continuity in fractured reservoirs, only the formation of a nodoid with a neck might be helpful due to positive capillary pressure. Other types of liquid bridge shape, i.e. catenoid (with zero capillary pressure) and unduloid (with negative capillary pressure), correspond to larger fracture apertures and are considered inefficient for capillary continuity. In addition, the unduloid-shaped liquid bridge spans a small range in Figure 12, which reveals that negative values of capillary pressure are relatively small because liquid bridges de-stabilize before reaching significant negative values. Hence, according to Figure 12, for thin fracture apertures, α=1 could be a good estimation for calculating the inner radius of curvature in Equation 4.

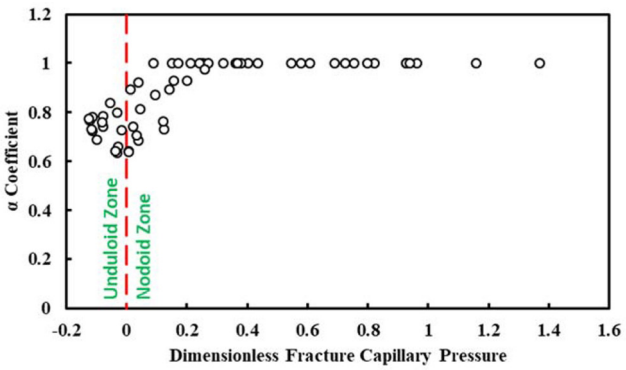

Fig. 12 α coefficient as a function of dimensionless fracture capillary pressure.

Capillary Force of Liquid Bridge

The formation of a liquid bridge between two solid bodies creates an attraction force between the solid supporting bodies. Different stability regions of the liquid bridge were distinguished based on the values of net capillary force by Dejam et al. [33]. Net capillary force is a sum of contributions from surface tension and fractures capillary pressure, and it was calculated by using the following expression [45]:

$$F_c = -\pi(2r_0\sigma + r_0^2 P_c) \quad (5)$$

Negative and positive values of Fc illustrate the state of attraction and repulsion between the two supporting plates, respectively. The capillary force between two plates versus fracture aperture for constant wettability and liquid bridge volume is shown in Figure 13. It could be seen that surface tension causes attraction between two supporting plates, whereas capillary pressure might impose attraction and repulsion for positive and negative values of capillary pressure, respectively. Due to negative values of capillary pressure, the repulsion force occurs in thicker apertures, very near to rupture. As a result, the absolute value of repulsion force due to capillary pressure is trivial. In addition, the net capillary force was negative for all apertures, so the formation of liquid bridges is accompanied by the attraction between the plates. In Figure 13, it is also demonstrated that the liquid bridge instability occurs when still a small amount of attraction is present between solid substrates. Then, in thicker fractures, although the fracture capillary pressure is zero or negative, the existence of a liquid bridge imposes an attraction force. The role of this attraction force on the capillary continuity needs further investigation. Theoretically, negative fracture capillary pressure tends to increase the pressure of the oil phase in the fracture hindering the oil drainage from the matrix block and provoking re-imbibition of oil into lower matrix blocks. Therefore, a liquid bridge with negative capillary pressure has no positive effect on maintaining capillary continuity, but it could promote liquid reinfiltration.

Prediction of Liquid Bridge Formation

The formation of a liquid bridge inside a horizontal fracture requires that the draining liquid drop from the upper matrix block reaches the lower surface of the fracture before rupture. The formed liquid bridge will be stable in the fracture if stability conditions are satisfied according to Equation 3, as presented in the section “Critical Fracture Aperture.”

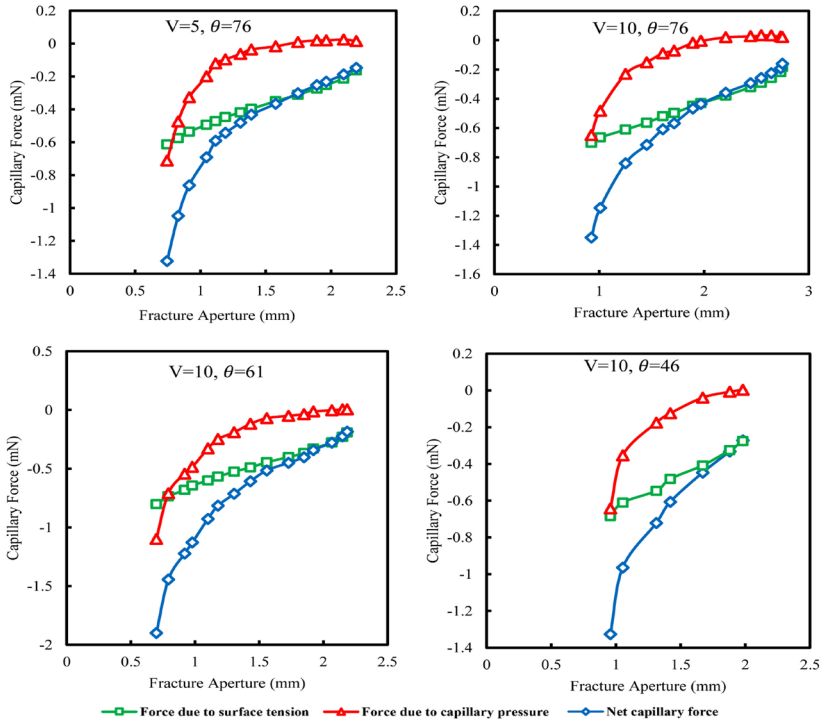

Fig. 13 Liquid bridge capillary force versus fracture aperture for different values of contact angle and liquid volume.

This equation only evaluates the stability of a formed liquid bridge inside the fracture, but it does not involve flow-related parameters, including liquid influx rate from the upper matrix block into the fracture and liquid viscosity. This section applies a mathematical model of one-dimensional elongation of liquid threads to develop relationships for better prediction of liquid bridge formation, including dynamic flow parameters.

A one-dimensional axisymmetric model was developed for a growing liquid drop dripping from a narrow tube until rupture by Wilson [46]. This model holds gravity, viscosity, and surface tension forces, ignoring inertia and assuming a constant influx rate. Wilson derived an equation for the breakage time, t_c, that could be used to find the maximum volume of liquid drop before rupture as: $V=Q.t_c$. However, this equation is implicit in breakage time, and therefore, it needs to be solved iteratively by numerical methods. As an alternative, the following approximate solution could be used to estimate breakage time:

$$t_{Dc}=(3\delta+0.42) \quad (6)$$

where t_{Dc} is dimensionless breakage time, $t_{D_c}=t_c/\sqrt{(\mu A0/\rho gQ)}$ and δ is a dimensionless parameter defined as $\delta=\sigma/\sqrt{\pi/(9\mu\rho gQ)}$. A similar, but not the same, the relationship was also previously proposed by Dejam and Hassanzadeh [32]. As shown in Figure 14, dimensionless breakage time could be accurately predicted by the proposed approximate solution. Now, using Equation 6, the following equation is obtained for predicting the maximum (or critical) volume of liquid drop before rupture:

$$V_c=Q(\frac{\mu A_0}{\rho gQ})^{0.5}(3\sigma(\frac{\pi}{9\mu\rho gQ})^{0.5}+0.42) \quad (7)$$

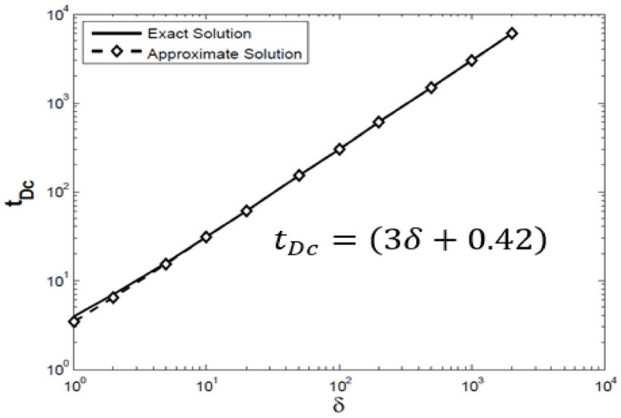

Fig. 14 Exact and approximate solutions of dimensionless rupture time, t_{Dc}

The above equation could be rewritten in terms of dimensionless Bond number (Bo) and Capillary number (Ca), as follows:

$$V_c=\pi(\frac{1}{Bo})+0.42(\frac{Ca}{Bo})^{0.5})r_c^3 \quad (8)$$

Where the dimensionless numbers are defined as $Bo=\rho g r_c^2/\sigma$ and $Ca=\mu u/\sigma$. By inserting Equation 8 in Equation 3, the following equation is found that relates critical fracture aperture to wettability and dynamic flow parameters:

$$b_{Dc}=0.674(1+1.37\theta)((\frac{1}{Bo})+0.42(\frac{Ca}{Bo})^{0.5})^{1/3} \quad (9)$$

where $b_{Dc}=b_c/r_c$ is dimensionless critical fracture aperture. Equation 9 states the maximum fracture aperture that could retain a stable liquid bridge formed from a liquid thread at its critical condition. In Figure 15, the dimensionless critical fracture aperture is presented as a function of the critical Bond number and Capillary number at a constant contact angle.

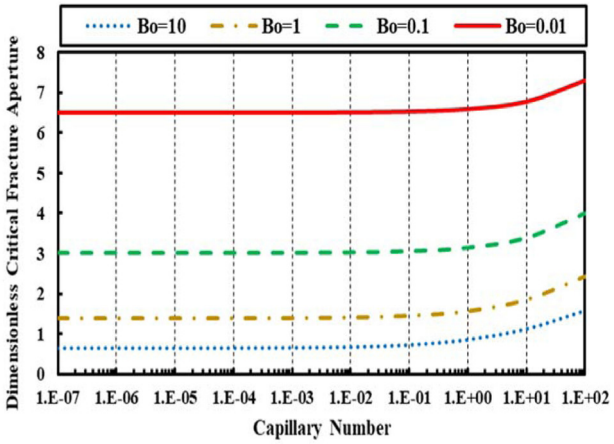

Fig. 15 Dimensionless critical fracture aperture as a function of capillary number for different values of critical Bond number.

In a given Bond number, critical fracture aperture is invariant with a capillary number for capillary number values less than about 0.001. On the other hand, Bond number, the ratio of surface tension to gravity force, affects the critical fracture aperture noticeably. As shown in Figure 15, dimensionless fracture aperture decreases with an increase in Bond number, which indicates that surface tension facilitates the stability of the liquid bridge, whereas gravity deteriorates its stability. Because the capillary number is usually smaller than 10-5 under reservoir conditions, and the Bond number ranges between 0.01 and 10, the Capillary to Bond number ratio is trivial [47]. Therefore, by ignoring the Ca/Bo term, Equation 8 is simplified to:

$$b_{Dc} = \frac{0.674(1+1.37\theta)}{Bo^{1/3}} \quad (10)$$

Using Equation 10, dimensionless critical fracture aperture versus contact angle for different values of Bond number is depicted in Figure 16. This figure again emphasizes that lower wetting tendency of the fracture surface, i.e. greater contact angles, improves bridge stability while increasing Bond number negatively affects bridge stability. Estimation of flow velocity into a single liquid thread is practically impossible. Thus, Equation 10 has superiority over Equation 9 since it does not need the value of the Capillary number. Hence, Equation 10 could provide an initial estimation of critical fracture aperture that only needs contact angle, contact radius and liquid properties.

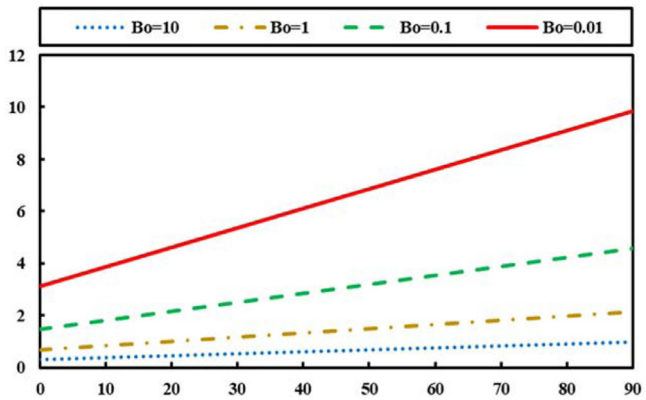

Fig. 16 Dimensionless critical fracture aperture as a function of contact angle for different values of critical Bond number.

Conclusions

In this study, the stability and capillary pressure of liquid bridges are investigated via laboratory experiments and mathematical modelling. The obtained experimental results are analyzed to interpret critical fracture aperture and fracture capillary pressure. The main finding of this study are summarized as follows:

• It has been found that the critical fracture aperture of a static liquid bridge is linearly proportional to the contact angle and the third root of liquid volume. Accordingly, a new expression is developed to predict the stability of static liquid bridges in fractures that predict the experimental results very well.

• A new method to evaluate the fracture capillary pressure from the experimentally measured profile of a liquid bridge was proposed based on the exact solution of the Young-Laplace equation.

• The results showed that fracture capillary pressure might be a positive or negative value depending on the fracture aperture. Only nodoid shaped liquid bridge with a neck yields positive capillary pressure that is responsible for capillary continuity. In addition, the fracture capillary pressure increases by decreasing fracture aperture for the whole range of bridge volume and wettability conditions.

• Calculations of capillary force showed that instability of liquid bridges occurs at small negative values of capillary force where still some attraction force exists.

•Using the 1D model of liquid dripping, a semi-analytical equation is obtained to predict critical fracture aperture, including gravity, viscous, surface tension, and wettability.

References

1. Aghabarari A, Ghaedi M (2019) A new simulation approach to investigate reinfiltration phenomenon in fractured porous media, Journal of Petroleum Science and Engineering, 181: 106182.
2. Aghabarari A, Ghaedi M, Riazi M (2020) Prediction of oil recovery in naturally fractured reservoirs subjected to reinfiltration during gravity drainage using a new scaling equation, Petroleum Exploration and Development, 47, 6: 1307-1315.
3. Firoozabadi A, Markeset T (1992) Laboratory study of reinfiltration for gas-liquid system in fractured porous media, presented at the SPE Annual Technical Conference and Exhibition, Washington, USA.
4. Sajjadian V, Danesh A, Tehrani D (1999) Laboratory study of gravity drainage mechanism in fractured carbonate reservoir-reinfiltration, presented at the SPE Latin American and Caribbean Petroleum Engineering Conference, Caracas, Venezuela.
5. Zobeidi K, Rasaei M-R, Fassihi M R (2015) Simulation of the experimental results of miscible gravity drainage performance in a stack of matrix blocks, Journal of Porous Media, 18, 11.
6. Gao S, Jin L, Du J, Liu H (2011) The liquid-bridge with large gap in micro structural systems, Journal of Modern Physics, 2, 05: 404.
7. Behrend O, Oulevey F, Gourdon D, Dupas E, Kulik A, Gremaud G, Burnham N (1998) Intermittent contact: tapping or hammering?, Applied Physics A, 66, 1: 219-221.

8. Dutka F, Napiórkowski M (2006) Formation of capillary bridges in two-dimensional atomic force microscope-like geometry, The Journal of Chemical Physics, 124, 12: 121101.
9. Mate C M, Novotny V (1991) Molecular conformation and disjoining pressure of polymeric liquid films, The Journal of Chemical Physics, 94, 12: 8420-8427.
10. Men Y, Zhang X, Wang W (2009) Capillary liquid bridges in atomic force microscopy: Formation, rupture, and hysteresis, The Journal of Chemical Physics, 131, 18: 184702.
11. Suzuki H, Mashiko S (1998) Adhesive force mapping of friction-transferred PTFE film surface, Applied Physics A: Materials Science and Processing, 66, 7: 1271-1274.
12. Stifter T, Marti O, Bhushan B (2000) Theoretical investigation of the distance dependence of capillary and van der Waals forces in scanning force microscopy, Physical Review B, 62, 20: 13667.
13. Alencar A M, Majumdar A, Hantos Z, Buldyrev S V, Stanley H E, Suki B (2005) Crackles and instabilities during lung inflation, Physica A: Statistical Mechanics and its Applications, 357, 1: 18-26.
14. DiLisi G, Dempsey R, Rarick R, Rosenblatt C (2015) Using parabolic flights to examine quantitatively the stability of liquid bridges under varying total body force, Microgravity Science and Technology, 27, 3: 145-153.
15. Pampaloni F, Reynaud E G, Stelzer E H (2007) The third dimension bridges the gap between cell culture and live tissue, Nature reviews Molecular Cell Biology, 8, 10: 839-845.
16. Delenne J-Y, Richefeu V, Radjai F (2013) Capillary states of granular materials in the funicular state, AIP Conference Proceedings, Montpellier, France, 1023-1026.
17. Iveson S, Litster J (1998) Fundamental studies of granule consolidation part 2: quantifying the effects of particle and binder properties, Powder Technology, 99, 3: 243-250.
18. Iveson S, Litster J (1998) Liquid-bound granule impact deformation and coefficient of restitution, Powder technology, 99, 3: 234-242.
19. Simons S J (2007) Liquid bridges in granules, Handbook of powder technology, Elsevier Science B.V., 1257-1316.
20. McFarlane J, Tabor D (1950) Adhesion of solids and the effect of surface films, Proceedings of the Royal Society of London. Series A. Mathematical and Physical Sciences, 202, 1069: 224-243.
21. Rabinovich Y I, Adler J J, Esayanur M S, Ata A, Singh R K, Moudgil B M (2002) Capillary forces between surfaces with nanoscale roughness, Advances in Colloid And Interface Science, 96, 1-3: 213-230.
22. Schubert H (1984) Capillary forces-modeling and application in particulate technology, Powder technology, 37, 1: 105-116.
23. Obata K J, Motokado T, Saito S, Takahashi K (2004) A scheme for micro-manipulation based on capillary force, Journal of Fluid Mechanics, 498: 113.
24. Piner R D, Zhu J, Xu F, Hong S, Mirkin C A (1999) " Dip-pen" nanolithography, Science, 283, 5402: 661-663.
25. Benard P, Zarebanadkouki M, Brax M, Kaltenbach R, Jerjen I, Marone F, Couradeau E, Felde V J, Kaestner A, Carminati A (2019) Microhydrological niches in soils: How mucilage and EPS alter the biophysical properties of the rhizosphere and other biological hotspots, Vadose Zone Journal, 18, 1: 1-10.
26. Benard P, Zarebanadkouki M, Hedwig C, Holz M, Ahmed M A, Carminati A (2018) Pore-scale distribution of mucilage affecting water repellency in the rhizosphere, Vadose Zone Journal, 17, 1: 1-9.
27. Carminati A, Benard P, Ahmed M A, Zarebanadkouki M (2017) Liquid bridges at the root-soil interface, Plant and Soil, 417, 1: 1-15.
28. Harimi B, Ghazanfari M H, Masihi M (2020) Modeling of capillary pressure in horizontal rough-walled fractures in the presence of liquid bridges, Journal of Petroleum Science and Engineering, 185: 106642.
29. Harimi B, Ghazanfari M H, Masihi M (2021) Analysis of evaporating liquid bridge in horizontal fractures, Journal of Petroleum Science and Engineering, 202: 108577.
30. Firoozabadi A, Hauge J (1990) Capillary Pressure in Fractured Porous Media (includes associated papers 21892 and 22212), Journal of Petroleum Technology, 42, 06: 784-791.
31. Mashayekhizadeh V, Kharrat R, Ghazanfari M, Dejam M (2012) An experimental investigation of fracture tilt angle effects on frequency and stability of liquid bridges in fractured porous media, Petroleum Science and Technology, 30, 8: 807-816.
32. Dejam M, Hassanzadeh H (2011) Formation of liquid bridges between porous matrix blocks, AIChE journal, 57, 2: 286-298.
33. Dejam M, Hassanzadeh H, Chen Z (2015) Capillary forces between two parallel plates connected by a liquid bridge, Journal of Porous Media, 18, 3: 179-188.
34. Miri R, Shadizadeh S, Kharrat R (2015) Static Stability of Liquid Bridges Between Matrix Blocks of a Gas Invaded Zone of Naturally Fractured Reservoirs, Petroleum Science and Technology, 33, 17-18: 1541-1551.
35. Bina O, Aminshahidy B, Dadvar M, Moghadasi J (2020) Capillary continuity in fractured porous media; part II: Evaluation of fracture capillary pressure in the presence of liquid bridges using a novel microfluidic approach, Journal of Molecular Liquids, 314: 113666.
36. Harimi B, Masihi M, Ghazanfari M H (2020) An insight into the formation of liquid bridge and its role on fracture capillary pressure during gravity drainage in fractured porous media, The Canadian Journal of Chemical Engineering, 99, S1: S212-S231.
37. Butt H-J, Kappl M (2010) Capillary Forces, Surface and interfacial forces, John Wiley and Sons, 127-161.
38. Dindoruk B, Firoozabadi A (1994) Computation of gas-liquid drainage in fractured porous media recognizing fracture liquid flow, SPE Annual Technical Meeting, Calgary, Alberta.
39. Dejam M (2018) The role of fracture capillary pressure on the block-to-block interaction process, Journal of Porous Media, 21, 11: 1121-1136.
40. Dehghan Monfared A, Ghazanfari M H, Jamialahmadi M, Helalizadeh A (2016) Potential application of silica

nanoparticles for wettability alteration of oil–wet calcite: A mechanistic study, Energy and Fuels, 30, 5: 3947-3961.
41. Mihajlović S, Sekulić Ž, Daković A, Vučinić D, Jovanović V, Stojanović J (2009) Surface properties of natural calcite filler treated with stearic acid, Ceramics–Silikáty, 53, 4: 268-275.
42. Fortes M (1982) Axisymmetric liquid bridges between parallel plates, Journal of Colloid and Interface Science, 88, 2: 338-352.
43. Lian G, Thornton C, Adams M J (1993) A theoretical study of the liquid bridge forces between two rigid spherical bodies, Journal of Colloid and Interface Science, 161, 1: 138-147.
44. Plateau J A F (1873) Statique expérimentale et théorique des liquides soumis aux seules forces moléculaires, Gauthier-Villars.
45. Kralchevsky P, Nagayama K (2001) Particles at fluid interfaces and membranes: attachment of colloid particles and proteins to interfaces and formation of two-dimensional arrays, Elsevier.
46. Wilson S (1988) The slow dripping of a viscous fluid, Journal of Fluid Mechanics, 190: 561-570.
47. Green D W, Willhite G P (1998) Enhanced oil recovery, Society of Petroleum Engineers, Richardson, Texas.